Preprint
UCRL-JC-137691

Modeling and demonstration of a saturated Ni-like Mo X-ray laser

J. Nilsen, Y. Li, J. Dunn, T.W. Barbee, Jr., and A.L. Osterheld

This article was submitted to
7th International Conference on X-ray Lasers, Saint-Malo, France, June 19-23,2000

August 21, 2000

U.S. Department of Energy
Lawrence Livermore National Laboratory

Approved for public release; further dissemination unlimited

DISCLAIMER

This document was prepared as an account of work sponsored by an agency of the United States Government. Neither the United States Government nor the University of California nor any of their employees, makes any warranty, express or implied, or assumes any legal liability or responsibility for the accuracy, completeness, or usefulness of any information, apparatus, product, or process disclosed, or represents that its use would not infringe privately owned rights. Reference herein to any specific commercial product, process, or service by trade name, trademark, manufacturer, or otherwise, does not necessarily constitute or imply its endorsement, recommendation, or favoring by the United States Government or the University of California. The views and opinions of authors expressed herein do not necessarily state or reflect those of the United States Government or the University of California, and shall not be used for advertising or product endorsement purposes.

This is a preprint of a paper intended for publication in a journal or proceedings. Since changes may be made before publication, this preprint is made available with the understanding that it will not be cited or reproduced without the permission of the author.

This report has been reproduced
directly from the best available copy.

Available to DOE and DOE contractors from the
Office of Scientific and Technical Information
P.O. Box 62, Oak Ridge, TN 37831
Prices available from (423) 576-8401
http://apollo.osti.gov/bridge/

Available to the public from the
National Technical Information Service
U.S. Department of Commerce
5285 Port Royal Rd.,
Springfield, VA 22161
http://www.ntis.gov/

OR

Lawrence Livermore National Laboratory
Technical Information Department's Digital Library
http://www.llnl.gov/tid/Library.html

Modeling and demonstration of a saturated Ni-like Mo X-ray laser

Joseph Nilsen, Yuelin Li*, James Dunn, Troy W. Barbee, Jr., and Albert L. Osterheld

Lawrence Livermore National Laboratory, Livermore, CA 94550

Abstract. The technique of using a nsec pulse to preform and ionize the plasma followed by a psec pulse to heat the plasma has enabled us to achieve saturated laser output for low-Z neon-like and nickel-like ions driven by small lasers with less than ten joules of energy. In this work we present and model recent experiments done using the COMET laser at Lawrence Livermore National Laboratory to illuminate slab targets of Mo up to 1 cm long with a one joule, 600 ps prepulse followed 700 psec later by a five joule, one psec drive pulse. The experiments demonstrate saturated output on the Ni-like Mo $3d^9 4d\ ^1S_0 \rightarrow 3d^9 4p\ ^1P_1$ laser line at 18.9 nm. The small signal gain and gain length product are estimated by measuring the laser output versus target length. Experiments are done using multilayer mirrors to obtain two-dimensional images of the output aperture of the laser and to measure the total laser energy as a function of various parameters such as the delay between the short and long pulses and the energy of the two pulses. To model the experiments the LASNEX code is used to calculate the hydrodynamic evolution of the plasma and provide the temperatures and densities to the XRASER code, which then does the kinetics calculations to determine the gain. The temporal and spatial evolution of the plasma is studied both with and without radiation transport included for the 4f and 4p $\rightarrow$ 3d Ni-like Mo resonance lines. High gains are predicted for both the $3d^9 4d\ ^1S_0 \rightarrow 3d^9 4p\ ^1P_1$ laser line at 18.9 nm and the $3d^9 4f\ ^1P_1 \rightarrow 3d^9 4d\ ^1P_1$ photopumped line which is observed to lase at 22.6 nm.

1. Introduction

Most researchers today use some variant of the prepulse technique [1-2] to achieve lasing in Ne-like or Ni-like ions. As a result the Ne-like $3p\ ^1S_0 \rightarrow 3s\ ^1P_1$ laser line now dominates the laser output as was predicted two decades ago. This technique illuminate solid targets with several pulses. The first pulse is used to create a large-scale length plasma, which is in the correct density range for gain and has sufficiently small density gradients for laser propagation. The subsequent pulses are then absorbed more efficiently and heat the plasma to lasing conditions. Typical pulse durations range from 100 ps to 1 ns and typically use 100 to 1000 J of energy. In the above techniques the pulse duration is held constant but the contrast and separation between pulses is varied. A recent variant of these techniques is the use of a nsec prepulse followed by a psec drive pulse. This approach was first used to demonstrate lasing at 32.6 nm in Ne-like Ti at the Max Born Institute (MBI) [3] using less than 10 joules of energy. The Ti experiments were reproduced at Lawrence Livermore National Laboratory (LLNL) using the COMET laser and extended to Ni-like Pd at 14.6 nm [4] and very recently to Ni-like Mo at 18.9 nm [5]. In this paper we present experiments that demonstrate saturated output on the Ni-like Mo $3d^9 4d\ ^1S_0 \rightarrow 3d^9 4p\ ^1P_1$ laser line at 18.9 nm. The small signal gain and gain length product are estimated by measuring the

laser output versus target length. Experiments are done using multilayer mirrors to obtain two-dimensional images of the output aperture of the laser and to measure the total laser energy as a function of various parameters such as the delay between the short and long pulses and the energy of the two pulses. We also model the Ni-like Mo experiments done with the COMET laser to understand the plasma conditions present and what gain is possible on different transitions. For Ni-like Mo we calculate lasing on both the 4d $^1S_0 \rightarrow$ 4p $^1P_1$ line at 18.9 nm and the 4f $^1P_1 \rightarrow$ 4d $^1P_1$ line at 22.6 nm. For the 4f $^1P_1 \rightarrow$ 4d $^1P_1$ line we discuss the role of the photopumping mechanism and present the measured gain for this line.

2. Plasma Modeling

To estimate what gain might be achieved on various transitions in Ni-like Mo we did LASNEX one dimensional (1D) computer simulations to model a Mo slab illuminated by a 1 J, 600 psec gaussian pulse followed 700 psec later by a 5 J, 1 psec gaussian pulse from a 1.05 μm Nd laser. The laser is focused to a 120 μm wide by 1.2-cm long line. The 700 psec delay between the long and short pulse is peak to peak. This is similar to the conditions used to demonstrate lasing in Ni-like Mo at the COMET laser facility. The LASNEX calculations include an expansion angle of 15 degrees in the dimension perpendicular to the primary expansion so as to simulate 2D effects.

Using the LASNEX calculated densities and temperatures as input to the XRASER code, the gains of the laser lines were calculated including radiation trapping effects for the four strong 4f and 4p $\rightarrow$ 3d resonance lines in Ni-like Mo. Bulk Doppler effects due to the expansion of the plasmas were also included. The XRASER atomic model includes all 107 detailed levels for levels up to n = 4 in Ni-like Mo.

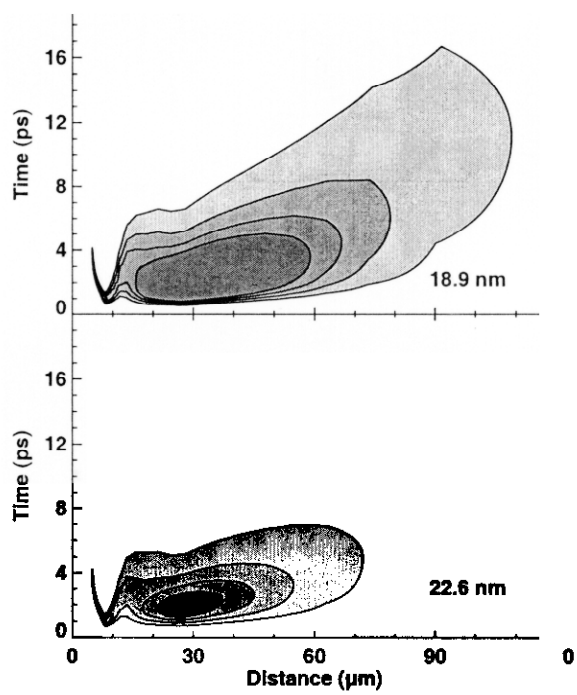

Fig. 1. Spatial and temporal evolution of the gain for the Ni-like Mo laser lines at 18.9 and 22.6 nm. Contours represent gain values greater than 120, 90, 60, and 30 cm^{-1}, respectively. Line transfer is included in this calculation. The short pulse laser drive peaks at 1 ps on this time scale.

Calculations predict two dominant laser lines that can be divided into two classes. First there is the 4d $^1S_0 \rightarrow$ 4p $^1P_1$ line at 18.9 nm that is populated by monopole collisional excitation of the Ni-like ground state. The other strong line is the 4f $^1P_1 \rightarrow$ 4d $^1P_1$ line at 22.6 nm that is populated primarily by photopumping on the strong 3d $^1S_0 \rightarrow$ 4f $^1P_1$ transition.

Figure 1 shows contours of the gain versus space and time for the 18.9 and 22.6 nm laser lines for the nominal drive conditions described above. The short pulse laser peaks at 1 psec on this time scale so the evolution during the long pulse is not shown. The horizontal axis gives the distance from the target surface in the direction of the plasma expansion. The gain contours, from darkest to lightest, represent gains greater than 120, 90, 60, and 30 cm^{-1}. The highest gain for the 18.9 nm line exceeds 300 cm^{-1} at a distance of 28 μm from the surface and at a time of 2 ps, which is just after the time of peak illumination. However this gain region is near the critical density surface and has steep gradients, which would make it difficult to propagate any significant distance. Looking at the electron density gradients it appears that the region that is more than 45 μm from the surface should allow good propagation. If we look at 50 μm from the surface the gain peaks at 3 ps with a value of 170 cm^{-1}. Gain > 30 cm^{-1} persists until 10 ps. The simulations show that the 22.6 nm line also has very strong gain but is more confined in space and time. Therefore we expect the spatially averaged gain for this line will be lower.

To give an idea of the plasma conditions we can look 50 μm from the surface at a time of 6 ps. The electron density is 6.4 x 10^{19} cm^{-3} with an electron temperature of 295 eV and an ion temperature of 47 eV. The gain on the 18.9 and 22.6 nm laser lines are 90 and 38 cm^{-1} respectively. The gradient in the electron density is -1.7 x 10^{22} cm^{-4}. This gradient would only refract the 18.9 nm laser line by 14 μm away from the target surface as it propagated over a 1 cm distance.

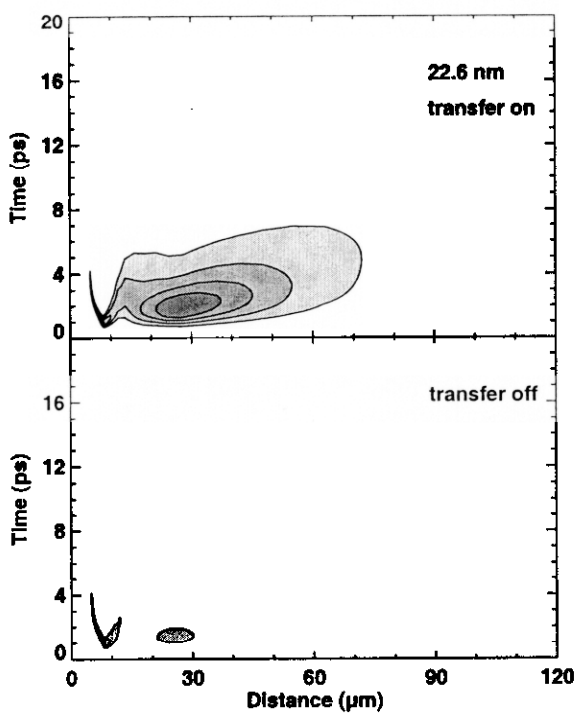

Fig. 2. Spatial and temporal evolution of the gain for the Ni-like Mo 4f → 4d laser line at 22.6 nm for the cases with the line transfer turned on and off. With the line transfer off the gain disappears. This shows the dramatic effect that photopumping has on driving the gain in this laser line. The short pulse laser drive peaks at 1 ps on this time scale. Contours represent gain values greater than 120, 90, 60, and 30 cm^{-1}, respectively.

One would normally not expect gain on the 4f → 4d laser line at 22.6 nm because its upper laser state is the 4f $^1P_1$ level which is depopulated by the rapid radiative decay to the ground state via the strongest resonance line. However, in this plasma, the 3d $^1S_0$ → 4f $^1P_1$ line is optically thick and radiation trapping allows a very large radiation field to build up on this line and therefore populate the 4f $^1P_1$ upper laser state by the self-photopumping process. To understand the role of the self-photopumping process on the gain of the Ni-like Mo laser lines, we did the XRASER calculations with the line transfer package turned off so that all the n = 4 → n = 3 resonance lines are optically thin and the self-photopumping process is absent. For the 18.9 nm laser line there is a modest reduction in the gain. For the 22.6 nm laser line, Fig. 2 shows contours of the gain with line transfer on and off. The gain contours, from darkest to lightest, represent gains greater than 120, 90, 60, and 30 cm^{-1}. The gain of the 22.6 nm laser line disappears without the photopumping process except for a very small region near the critical density surface. This clearly shows that photopumping is the mechanism that drives this line. A detailed analysis of the photopumping for the analogous 3d → 3p line in Ni-like Ti can be found in Ref. [6].

One issue that needs to be addressed is the difference between the laser system driven with 100 ps pulses versus those driven with 1 ps pulses. Since we have only begun to model the Ni-like Mo and we have done much more extensive modeling for Ne-like Ti we would like to briefly discuss the transient nature of the Ne-like Ti laser. From our modeling of the Ti laser driven by a 1 ps pulse we would characterized the lasing on the neon-like titanium lines at 32.6 and 30.1 nm as quasi steady state. The heating time is shorter than the ionization time but longer than the equilibration time for the upper laser states. The big difference between driving a titanium plasma with a 1 psec pulse versus a 100 psec pulse is the comparison with the ionization time. For the 1 psec pulse one expects the plasma to lase after the psec drive while with a 100 psec pulse one would expect the lasing on the rising edge of the pulse before the neon-like stage has been completely ionized. The modeling of the Ne-like Ti is described in great detail in Ref. [6]. We expect similar behavior in Ni-like Mo.

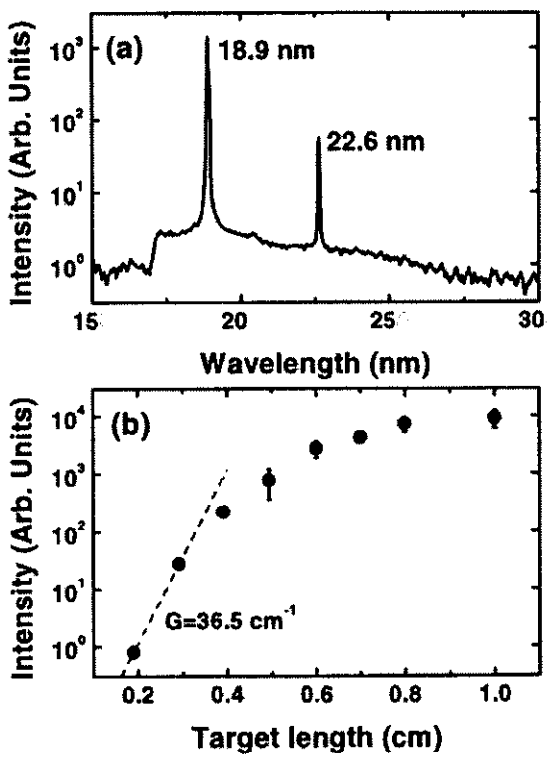

Fig. 3. (a) Intensity versus wavelength for a 1-cm long Mo target shows lasing on the 18.9 nm and 22.6 nm Ni-like Mo lines; (b) Intensity versus target length for the Ni-like Mo 18.9 nm laser line. The small signal gain is measured to be 36.5 cm^{-1} with an overall gain-length product of 16.6 as the laser line saturates. The long pulse and short pulse energies were 1.1 J and 5.0 J, respectively, with a 700 ps delay.

3. Experiments

Saturated operation of the Ni-like Mo X-ray laser was demonstrated on the compact multipulse terawatt (COMET) laser system at LLNL. A 600 ps long pulse and a 1 ps short pulse beam from a table-top, 1.053 μm Ti:Sapphire-Nd:Glass hybrid chirped pulse amplification laser system are sent into the target chamber. The short pulse is focused on to the target to form an 80 μm by 1.1-cm line focus. The long pulse is defocused to be two times broader in order to ensure a better overlap with the short pulse and to produce a more uniform lateral plasma. The laser can be fired every 4 minutes so many experiments can be done each day. To more efficiently use the short-lived population inversion, we implemented a traveling wave excitation setup using a 5-segment stepped mirror. We did experiments to compare the X-ray laser output with and without the traveling wave. In the case without the traveling wave, the step mirror was replaced by a flat one.

We used both near field imaging and on-axis spectroscopy to investigate the X-ray laser performance. Normally, the x-ray laser output is sent to an on-axis flat field grating spectrometer that is coupled to a back-thinned, CCD and has wavelength coverage of 14 - 35 nm. The spectrometer gives time-integrated spectra with angular resolution in the plane of the normal of the target and the axis of the line focus. To do near-field imaging we use three Mo_2C/Si multilayer mirrors. The first mirror is spherical and images the output aperture of the X-ray laser onto a back-thinned X-ray CCD. The other 2 flat mirrors, one with normal and the other with 45° incidence, fold the beam to obtain a magnification of 14.1. With the 24-μm pixels of the CCD, this gives a spatial resolution of 1.7 μm. The calculated total reflectivity of the multilayer imaging system is 5.9% with a bandwidth of 1 nm at 18.9 nm. To protect the multilayer mirrors from target debris, attenuate the X-ray laser intensity, and block the visible light, aluminum filters of various thickness were used. A more detailed description of the Ni-like Mo experiments can be found in Refs. [7-8].

Using the traveling wave geometry dramatically enhances the X-ray laser output by one to two orders of magnitude and makes the X-ray laser output less sensitive to the delay between the long and short pulse. For that reason we used the traveling wave geometry for all subsequent experiments. We did a series of experiments using the near-field imaging system to determine that a delay of 700 ps works well for the conditions we are using.

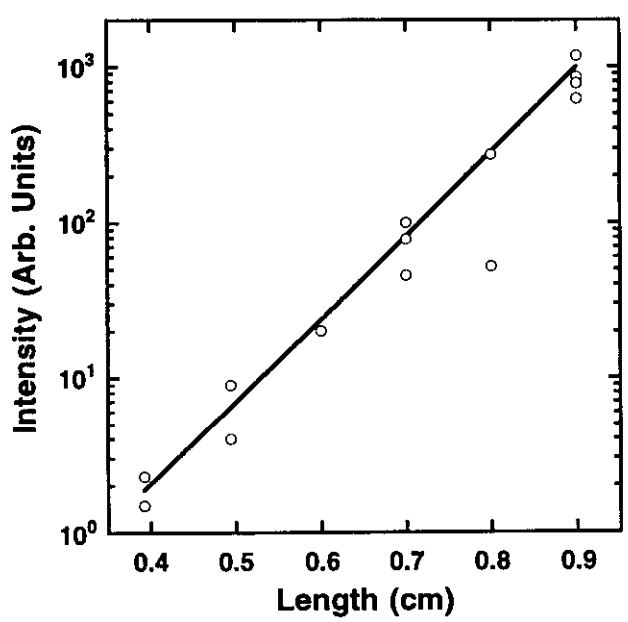

Fig. 4. Intensity versus length for the Ni-like Mo 22.6 nm laser line. The small signal gain is estimated to be 13 cm^{-1} with no indication of saturation. The long pulse and short pulse energies were 1.1 J and 5.0 J, respectively, with a 700 ps delay.

With this delay, Fig. 3(a) presents the spectrum for a full length target (1cm) that shows the two strong laser lines at 18.9 nm and 22.6 nm. We then varied the target length while holding the line focus constant to measure the small signal gain and estimate an overall gain-length product of 16.6 for the 18.9 nm line. From the measured intensity versus length shown in Fig. 3(b) we estimate the small signal gain of 36.5 cm^{-1} on the 18.9 nm line and believe this line has reached saturation intensity as the gain curve flattens out. For the 22.6 nm laser line Fig. 4 shows the intensity versus length from which we estimate a gain of 13 cm^{-1}. For this line we do not see any sign of saturation. Both the 18.9 and 22.6 nm laser lines are very robust to changes in laser conditions and allow good gain-length measurements to be made.

Using the near field imaging diagnostics we did many experiments to study the laser output as a function of the delay and contrast between the long and short pulse. We could also observe how the beam quality changed as a function of how many times we shot on the same target. From those experiments we could measure the absolute energy of the 18.9 nm laser line and verify independently that we had reached saturation. Fig. 5 shows a near field image of the 18.9 nm X-ray laser line which used 4 J in the long pulse and 5 J in the short pulse with a 700 ps delay. The optical laser is incident from the right with the vertical direction parallel to the target surface. The plasma expands in the horizontal direction. The absolute position of the target surface is uncertain but we estimate its position as 0 μm on the horizontal axis based on plasma emission. The FWHM of the lasing region is 90 μm in the vertical direction and 70 μm in the horizontal direction with peak emission about 30 μm from the target surface. The measured output energy is 2.3 μJ with an estimated intensity of 5 GW/cm^2. This exceeds the calculated saturation intensity of 2 – 3 GW/cm^2 estimated by our calculations. For the nominal case of 1 J in the long pulse the X-ray laser intensity is about one-half the value observed for the 4J long pulse but still reaches saturation intensity.

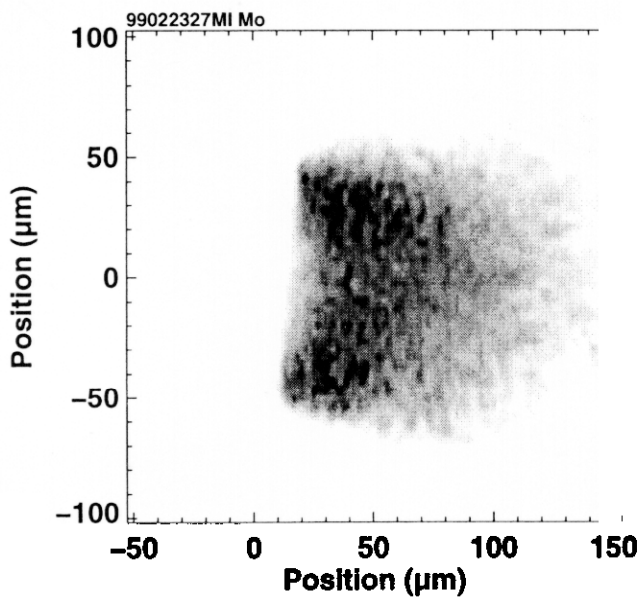

Fig. 5. Near-field image of the Ni-like Mo 18.9 nm laser line for a 1-cm target. The target surface is at 0 μm on the horizontal axis and the pump laser is incident from the right. The long and short pulse energies are 4 and 5 J, respectively, with a 700 ps delay between pulses. The total energy of the X-ray laser is estimated to be 2.3 μJ.

4. Conclusions

In this work we present and model recent experiments done using the COMET laser at Lawrence Livermore National Laboratory to illuminate slab targets of Mo up to 1 cm long with a 1 J, 600 ps prepulse followed 700 psec later by a 5 J, 1 psec drive pulse. The experiments demonstrate saturated output on the Ni-like Mo $3d^9 4d\ ^1S_0 \rightarrow 3d^9 4p\ ^1P_1$ laser line at 18.9 nm. The small signal gain and gain length product are estimated to be 36.5 cm^{-1} and 16.6 respectively, by measuring the laser output versus target length. Experiments were done using multilayer mirrors to obtain two-dimensional images of the output aperture of the laser and to measure the total laser energy as a function of various parameters such as the delay between the short and long pulses and the energy of the two pulses. We estimate an output energy of 2.3 μJ for the saturated laser.

To model the experiments the LASNEX code is used to calculate the hydrodynamic evolution of the plasma and provide the temperatures and densities to the XRASER code, which then does the kinetics calculations to determine the gain. The temporal and spatial evolution of the plasma is studied both with and without radiation transport included for the 4f and 4p → 3d Ni-like Mo resonance lines. High gains are predicted for both the $3d^9 4d\ ^1S_0 \rightarrow 3d^9 4p\ ^1P_1$ laser line at 18.9 nm and the $3d^9 4f\ ^1P_1 \rightarrow 3d^9 4d\ ^1P_1$ photopumped line at 22.6 nm. Gain of 13 cm^{-1} is measured for the photopumped line at 22.6 nm.

Acknowledgements – The authors would like to thank Richard Ward and Andi Hazi for their support. Yuelin Li acknowledges support from Hector Baldis of the Institute for Laser Science and Applications (ILSA). This work was performed under the auspices of the U.S. Department of Energy by the University of California Lawrence Livermore National Laboratory under contract No. W-7405-Eng-48.

* Yuelin Li is currently at Argonne National Laboratory, Argonne, IL 60439

References

[1] J. Nilsen, B. J. MacGowan, L. B. Da Silva, and J. C. Moreno, Phys. Rev. A **48**, 4682 (1993).
[2] J. Nilsen and J. C. Moreno, Phys. Rev. Lett. **74**, 3376 (1995).
[3] P. V. Nickles, V. N. Shlyaptsev, M. Kalachnikov, M. Schnuerer, I. Will, and W. Sandner, Phys. Rev. Lett. **78**, 2748 (1997).
[4] J. Dunn, A. L. Osterheld, R. Shepherd, W. E. White, V. N. Shlyaptsev, and R. E. Stewart, Phys. Rev. Lett. **80**, 2825 (1998).
[5] J. Dunn, J. Nilsen, A. L. Osterheld, Y. L. Li, and V. N. Shlyaptsev, Opt. Lett. **24**, 101 (1999).
[6] J. Nilsen, Y. L. Li, and J. Dunn, J. Opt. Soc. Am. B **17**, 1084 (2000).
[7] Y. L. Li, J. Dunn, J. Nilsen, T. W. Barbee, Jr., A. L. Osterheld, and V. N. Shlyaptsev, J. Opt. Soc. Am. B **17**, 1098 (2000).
[8] Y. L. Li, J. Dunn, J. Nilsen, T. W. Barbee Jr., L. B. Da Silva, A. L. Osterheld, and V. N. Shlyaptsev, "*Near field imaging of a saturated table top X-ray laser*," *SPIE Proceedings 3776 - Soft X-ray Lasers and Applications III*, edited by J. J. Rocca and L. B. Da Silva (SPIE Press, Bellingham, 1999), pp. 45 – 51